Symmetry restoration of HFB states using projection

Master Thesis

by
Carl Frostenson

Department of Physics, Mathematical Physics
Lund University

Supervisor Gillis Carlsson
Co-supervisor Andrea Idini
Examiner Sven Åberg

LUNDS
UNIVERSITET

June 26, 2019

Examensarbete för 30 hp Institutionen för fysik, Naturvetenskapliga fakulteten, Lunds universitet

Thesis for a diploma in Physics, 30 ECTS credits Department of Physics, Faculty of Science, Lund University

Abstract

The restoration of particle number and angular momentum symmetry using projection operators has been theoretically investigated for mean-field Hartree-Fock-Bogoliubov (HFB) states. A computer code for the projection of particle number was then implemented. To do so efficiently and avoid the sign ambiguity of the Onishi formula, the computation of overlap between quasi-particle vaccums using Pfaffians was investigated. Different algorithms for the the Pfaffian from [1],[2], was tested for performance and accuracy. For the same reason different truncations of the model space was also investigated. The particle number projector was then implemented in *HOSPHE* [3] for calculations of ground states pertaining to an effective Quadrupole plus Pairing Hamiltonian calculated using the SLy4 parametrization of the Skyrme interaction.

Populärvetenskaplig sammanfattning

Den vanligaste formen av materia i vårt universum består av elemntarpartiklar som kallas för kvarkar och leptoner. Dessa kvarkar attraherar varandra som en effekt av den starka och svaga växelverkan - som förmedlas genom utbytet av bosoner. I atomkärnan är det den starka växelverkan, vars effekt bärs av gluoner, som binder samman upp- och nerkvarkar till neutroner och protoner. Kombinationen av kvarkar, som också är elektrostatiskt laddade, gör i sin tur att protonen blir positivt laddad och neutronen oladdad. Den positiva laddning hos protonerna gör att atomkärnan kan binda elektroner till sig. Denna kombination av olika krafter eller växelverkan är orsaken bakom strukturen hos grundämnena i det periodiska systemet. Dessa grundämnen utgör majoriteten av den materia vi som människor på jorden kommer i direkt kontakt med på daglig basis.

Människan har sedan slutet av 1700-talet haft en god förståelse för den elektrostatiska Coulomb-växelverkan. Däremot har vi fortfarande inte en komplett beskrivning av den starka växelverkan som binder samman nukleoner. Detta är för att växelverkan mellan nukleoner, som egentligen är växelverkan mellan kvarkar, blir ett ökänt komplext flerpartikelproblem om det ska behandlas exakt. Den starka växelverkan mellan nukleoner kallas ofta för den starka kärnkraften och är en effektiv växelverkan, snarlikt van der Waals-kraft mellan atomer. Problemet med att beskriva denna växelverkan i form av en potential för flera interagerande nukleoner, som är fallet för en atomkärna, kan lösas approximativt på många sätt.

Ett vanligt sätt att lösa flerpartikelproblem i allmänhet är att införa så kallade medelfältsapproximationer, som möjliggör att interaktionen mellan N-partiklar kan separeras till N stycken enpartikelsproblem. För atomkärnor används ofta en metod lånad från fasta tillståndets fysik, där man studerar elektroners effektiva växelverkan. Denna metod kallas för BCS-metoden och tillåter parbildning, alltså att nukleoner binder till varandra. Med denna parbildning i åtanke kan man sedan behandla hela kärnan utifrån dessa par, istället för enskilda nukleoner. En effekt av denna metod är att symmetrier i systemet bryts, och man kan inte längre vara säker på att lösningarna, alltså ungefärliga beskrivningar av kärnan, innehåller ett korrekt antal nukleoner. Andra egenskaper som spin bevaras inte heller.

För att återinföra dessa symmetrier till kärnan används så kallade projektionsmetoder. I denna avhandling studeras dessa metoder för partikelantal- och spinprojektion. Vidare implementeras en datorkod som projicerar partikelantal genom att använda en så kallad Pfaffian. Olika metoder för att beräkna Pfaffianen studeras samt metoder för att snabba upp dess beräkning. Slutligen implementeras partikelantalsprojektionen i en mer realistisk beräkning för att se hur mycket närmare en korrekt beskriving av $^{18}_{8}$O denna symmetriåterföring åstadkommer.

Preface

This is the report for my 30 credit degree project in theoretical nuclear physics at the Department of Physics, Faculty of Science, at Lund university. The project was commenced in september of 2018 and completed in june 2019. The thesis is the concluding assignment of a Civil Engineering Degree in Engineering Physics at LTH, the Faculty of Engineering of Lund University. The specialization of my degree being theoretical physics naturally lead my interest to nuclear physics which resulted in this thesis.

I would like to thank my supervisors Gillis Carlsson and Andrea Idini for their great patience, physical insights, knowledgable advice and care. Without them this thesis would most definitely not be. I would also like to thank my office mates Ingemar Ragnarsson, Gunnar Ohlén and Paul André but also to my office neighbour Cecilia Jarlskog for their company and good-humored banter. They have raised my sprit in time of great need. I'm also grateful for the time and patience of Sven Åberg, my examiner. The encouragement and support from my family has been invaluable during this process. Finally I am deeply grateful towards Stina, my girlfriend, for her tremendous support and encouragement. Without her I would most definitely not be where I am today.

Contents

Chapter 1

Introduction

The ordinary matter in our universe is made up of elementary particles known as quarks and leptons; of which the up and down quarks together with the gluons create the nucleons. Nucleons and electrons aggregated form the atoms of the chemical elements found in nature. The electrons are bound to the nucleons by the coloumb force - an interaction that has been well described since 1785. The force keeping the nucleons together on the other hand, is the strong nuclear force. This interaction has not been given a final end-all-be-all potential, but models have been worked on since the beginning of nuclear physics. For larger many-body systems of nucleons the problem of a complete description of the interaction becomes even more challenging. By the introduction of mean-field approaches the N-body problem can be reduced to N single-particle systems. The solution of these fields leads, in the case of fermions, to product-state solutions of an anti-symmetrized Fock space called slater determinants. The most common way of optimising the mean-field is through the self-consistent variational principle of Hartee-Fock.

Analogous to electron systems with short-range particle-particle interactions leading to superconductive states, the introduction of Cooper-pairs in nuclei can further improve the mean-field solutions. This approach is called Hartee-Fock-Bogoliubov mean-field theory and is a very common strategy to computationally approach the nuclear many-body problem. Albeit being a powerful method, it yields a wave function that spontaneously breaks certain symmetries of the original Hamiltonian such as particle number and nuclear spin. Hence a way to increase the accuracy of the solution is to restore said symmetries, which is commonly done through the use of projection operators.

Another very common approach that also lends much of its theoretical background from electron systems is density functional theory. This approach uses effective interactions tuned to their purpose by mean-field calculations. In nuclear theory the structure of the effective interaction is often not derived ab-intio as is the case for electrons. Instead the shape is merely motivated ab-initio followed by comprehensive fitting of the parameters to structural data.

In this thesis the introduction of symmetry restoration through projection of HFB-states is studied. The theoretical framework for symmetry restoration of particle number projection as well as angular momentum using a variation after projection approach is outlined, together with a general generator coordinate method. Computations for restoration of particle number is implemented using Pfaffians for a BCS-model with seniority pairing, in HFB-formalism. Different Pfaffian routines are tested for performance using the metrics of runtime and relative error. Methods of truncating the model space for further computational optimization is investigated. Lastly particle number restoration is implemented in an extension of the program *HOSPHE*; these calculations map DFT-interactions to an effective Hamiltonian with pairing plus quadrupole deformation which is then solved using HFB mean-field variation where the resulting states are used for configuration mixing with deformation together with proton and neutron number as generator coordinates.

Chapter 2

Theory & Methodology

2.1 The Model space

The model space we start from is generated by the eigenstates of the BCS Hamiltonian using seniority pairing. This means we treat the pairing interaction G as a constant interaction between pairs of conjugate states $\{\alpha, \bar{\alpha}\}$ [4]. Hence we start from the following Hamiltonian:

$$H_{BCS} = \sum_{\alpha>0} \varepsilon_\alpha (c^\dagger_\alpha c_\alpha + c^\dagger_{\bar{\alpha}} c_{\bar{\alpha}}) - G \sum_{\alpha,\alpha'>0} c^\dagger_\alpha c^\dagger_{\bar{\alpha}} c_{\bar{\alpha'}} c_{\alpha'} \equiv H_{s.p.} + H_G \tag{2.1}$$

Where $c^\dagger_\alpha$ and $c_{\bar{\alpha}}$ are fermionic creation and annihilation operators for the state α. The sums α, α' runs over half the states, as for each state α there exists a conjugate state $\bar{\alpha}$, which in the case of BCS is the time-reversed state. The set of states $\{\alpha, \bar{\alpha}\}$ generate the whole model space[4]. The single particle energies ε_α are the eigenvalues of the spherical modified oscillator (MO) Hamiltonian also called the Nilsson model[5] (using ... to denote line break):

$$\begin{aligned} \varepsilon(N_{osc}, \ell, j) \equiv \hbar\omega_0 \Bigg[N_{osc} + \frac{3}{2} - \kappa \begin{cases} \ell \\ -(\ell+1) \end{cases} \quad \dots \\ \dots - \mu' \left(\ell(\ell+1) - \frac{N_{osc}(N_{osc}+3)}{2} \right) \Bigg] \begin{cases} j = \ell + 1/2 \\ j = \ell - 1/2 \end{cases} , \\ \hbar\omega_0^{\mathrm{N,Z}} \equiv 41 \cdot \mathrm{A}^{-1/3} \left(1 \pm \frac{1}{3} \frac{\mathrm{N} - \mathrm{Z}}{\mathrm{A}} \right) \text{ MeV}. \end{aligned} \tag{2.2}$$

N_{osc} is the principal quantum number, denoting the major oscillator shell, ℓ is the orbital angular momentum quantum number and $j = \ell + s$ is the total angular momentum (per nucleon) quantum number. As usual in the literature: N is the neutron number, Z is the proton number and A=N+Z is the atomic number. The values of the MO parameters (κ, μ') are chosen in accordance with [5]. κ is the strength of the spin-orbit or $\ell \cdot \mathbf{s}$-coupling and μ' is the strength of the ℓ^2-term.

The single particle states of H_{bcs} are found by the introduction of pairing operators,

$$P^\dagger \equiv \sum_{\alpha>0} c^\dagger_\alpha c^\dagger_{\bar{\alpha}}, \tag{2.3}$$

which create Cooper-pairs of particles coupling to $m_j = 0$. The pairing interaction can now be cast in a new form;

$$H_G = -GP^\dagger P, \tag{2.4}$$

which lends itself to a straightforward linearization giving a (mean-) pair field

$$H_\Delta = -\Delta(P^\dagger + P)\ ,\ \Delta \equiv G\left\langle P^\dagger \right\rangle . \tag{2.5}$$

Linearization of the pairing interaction:

$$\begin{aligned} H_G = -GP^\dagger P &= -G(P^\dagger - \left\langle P^\dagger \right\rangle + \left\langle P^\dagger \right\rangle)(P - \langle P\rangle + \langle P\rangle) \\ &= -G\left\langle P^\dagger \right\rangle (P^\dagger + P) - G(P^\dagger - \left\langle P^\dagger \right\rangle)(P - \langle P\rangle) + G\left\langle P^\dagger \right\rangle^2 \\ &\approx -G\left\langle P^\dagger \right\rangle (P^\dagger + P) \end{aligned}$$

where the third equality makes of $\langle P\rangle = \left\langle P^\dagger \right\rangle$ and the final approximation assumes that $P^\dagger \approx \left\langle P^\dagger \right\rangle$, $P \approx \langle P\rangle$ and $\left\langle P^\dagger \right\rangle^2 << 1$.

Replacing the original pairing interaction H_G by the pairing field or potential H_Δ the Hamiltonian is bilinear in the single particle creation operators $\{c^\dagger_\alpha, c_\alpha\}$. This fact was utilized by Bogoliubov and Valantin (1958) by a unitary transformation of these operators into quasi-particle operators given by

$$\begin{cases} b^\dagger_\alpha = U_\alpha c^\dagger_\alpha - V_\alpha c_{\bar{\alpha}} \\ b_\alpha = U_\alpha c_\alpha - V_\alpha c^\dagger_{\bar{\alpha}} \end{cases} , \begin{cases} b^\dagger_{\bar{\alpha}} = U_\alpha c^\dagger_{\bar{\alpha}} + V_\alpha c_\alpha \\ b_{\bar{\alpha}} = U_\alpha c_{\bar{\alpha}} + V_\alpha c^\dagger_\alpha \end{cases} . \tag{2.6}$$

These quasi-particle operators obey the standard fermionic anti-commutation relations. This rotation in the Fock-space yields a variational minimization problem where the parameters U_α, V_α must obey

$$|U_\alpha|^2 + |V_\alpha|^2 = 1, \tag{2.7}$$

if the solution is to be normalized. Using the time reversed states;

$$|\alpha\rangle = |nljm\rangle\ ,\ |\bar{\alpha}\rangle = |nlj - m\rangle\ ,\ m > 0, \tag{2.8}$$

gives the phase convention

$$U_\alpha = U_{\bar{\alpha}} > 0\ ,\ V_\alpha = -V_{\bar{\alpha}} > 0. \tag{2.9}$$

One can now identify the V^2_α as the occupation probability of the the state α, and U^2_α as the complementary probability of the state being unoccupied.

The resulting Hamiltonian no longer preserves particle number, but can be forced to do so on average by Langrange multiplier $-\lambda N$. The final Hamiltonian H' is then given as

$$H' = H_{\text{s.p.}} + H_\Delta - \lambda N, \tag{2.10}$$

where diagonalization gives the equation [4],[5]:

$$2U_\alpha V_\alpha(\varepsilon_\alpha - \lambda) - \Delta(U_\alpha^2 - V_\alpha)^2 = 0. \tag{2.11}$$

The physical solutions are then

$$U_\alpha = \left[\frac{1}{2}\left(1 + \frac{\varepsilon_\alpha - \lambda}{E_\alpha}\right)\right]^{1/2},$$
$$V_\alpha = \left[\frac{1}{2}\left(1 - \frac{\varepsilon_\alpha - \lambda}{E_\alpha}\right)\right]^{1/2},$$

with the quasi-particle energies:

$$E_\alpha \equiv \sqrt{(\varepsilon_\alpha - \lambda)^2 + \Delta^2}. \tag{2.12}$$

From (2.12) one can see that the ground state should have zero quasi-particles since E_α is a monotonous function of Δ. Denoting this quasi-particle vaccum by $|-\rangle$ it must obey

$$b_\alpha |-\rangle = b_{\bar{\alpha}} |-\rangle = 0 \quad \forall\, \alpha. \tag{2.13}$$

The quasi-particle vacuum can thus be constructed as

$$|-\rangle \propto \prod_\alpha b_\alpha b_{\bar{\alpha}} |0\rangle\,, \tag{2.14}$$

which transformed back into single particle operators of the MO is given as

$$|-\rangle = \prod_m \left(U_m + V_m c_{jm}^\dagger c_{j\bar{m}}^\dagger\right) |0\rangle\,. \tag{2.15}$$

Using the empirical relation for the pairing strength [5]:

$$\Delta_{emp} = \frac{12}{\sqrt{A}}\,\text{MeV}, \tag{2.16}$$

the U_k, V_k factors can be determined by a scan of λ until

$$\lambda = \langle N \rangle = \sum_{\alpha>0} 2V_\alpha^2 = \text{N/Z}. \tag{2.17}$$

The result of the these BCS calculations can then be cast in HFB formalism as

$$\begin{pmatrix} b^\dagger \\ b \end{pmatrix} = \mathcal{W}^\dagger \begin{pmatrix} c^\dagger \\ c \end{pmatrix}, \quad \mathcal{W} \equiv \begin{pmatrix} U & V^* \\ V & U^* \end{pmatrix} \in \mathbb{C}^{2n\times 2n}, \tag{2.18}$$

where $\mathbb{C}^{2n\times 2n}$ denotes the set of all complex $2n \times 2n$ matrices. From the definition of the Bogoliubov-Valantin transformation, forcing fermion commutation relations translates into [4]:

$$\mathcal{W}^\dagger \mathcal{W} = \mathcal{W}\mathcal{W}^\dagger = \mathbb{1}. \tag{2.19}$$

From the Bloch-Messiah theorem the form of $\mathcal{W}$ can be deduced. In the BCS formalism the density matrix is diagonalized to begin with and by choosing the time reversed states as the conjugate states the U, V matrices are given as:

$$U = \begin{pmatrix} U_1 & 0 & & \mathbf{0} \\ 0 & U_1 & & \\ & & \ddots & \\ \mathbf{0} & & & \begin{matrix} U_n & 0 \\ 0 & U_n \end{matrix} \end{pmatrix},$$

$$V = \begin{pmatrix} 0 & V_1 & & \mathbf{0} \\ -V_1 & 0 & & \\ & & \ddots & \\ \mathbf{0} & & & \begin{matrix} 0 & V_n \\ -V_n & 0 \end{matrix} \end{pmatrix}.$$

The above linearization of the pairing interaction into a mean field can be seen as a phase transition of the nuclei into a superfluid state. This approximation, as it turns out, is better the stronger the pairing interaction is. However, as stated above, the resulting Hamiltonian now breaks certain symmetries. This is equivalent to the Hamiltonian no longer commuting with the angular momentum operator nor the particle number operator[4]:

$$[H, N] \neq 0, \quad [H, J^2] \neq 0. \tag{2.20}$$

This means the ground-state solution obtained contains correlations with excited states. To remove these correlations and obtain better approximations of the true ground state a superposition of many-body wave functions i.e. slater determinants is used. This method of configuration mixing actually gives the exact ground state in the case of the BCS model, and greatly improves the calculations based on the DFT to Hamiltonian calculations.o

2.2 Projection operators

To restore the symmetry of the true Hamiltonian the projection operator method is utilized. The method of particle number symmetry involves the projection by abelian symmetry groups, whereas the angular momentum restoration utilize non-abelian symmetry groups. This makes the mathematical structure of the projectors different, which means the initial definition of the operators needs a rather different treatment. The mathematical framework behind both methods will be outlined in the following section.

In general a projection can be seen as an expansion of the wave function in the basis functions of the irreducible representation of the symmetry group. To find such an expansion one wish to construct a projection operator P^ν such that for any arbitrary state $|\Psi\rangle$ the action upon this state is the projection $P^\nu |\Psi\rangle$ into the irreducible subspace defined by the operator. Let $\{|\Phi^\nu\rangle\}$ be a basis of this irreducible subspace, these functions then transform as [6],[7]

$$R(g) |\Phi_i^\nu\rangle = \sum_j D_{ji}^\nu(g) \left|\Phi_j^\nu\right\rangle, \tag{2.21}$$

where g is the group element and $\{R(g)\}$ is the group transformations. The matrix functions $D_{ji}^\nu(g)$ are the single-valued representations of the group. For the rotation group in three dimensions $SU(3)$, they correspond to the so called Wigner D-functions. For the gauge rotation in particle number $U(1)$ they are simply $e^{-i\varphi N}$ [7],[8]. According to group representation these matrix representations must obey their own orthogonality relation

$$\frac{V}{n_\nu}\delta_{\nu\nu'}\delta_{ii'}\delta_{jj'} = \begin{cases} \sum_g D_{j'i'}^{\nu'*}(g) D_{ji}^\nu(g), \text{ for finite groups,} \\ \int dg D_{j'i'}^{\nu'*}(g) D_{ji}^\nu(g), \text{ for infinite groups} \end{cases}. \tag{2.22}$$

The number n_ν corresponds to the dimension of the irreducible representation and V , for finite groups is the order of the group, whereas for continuous groups it is the volume of the parameter space [6].

Multiplying equation (2.22) by $D_{j'i'}^{\nu'*}(g)$ and sum over the group gives:

$$\delta_{\nu\nu'}\delta_{jj'}\frac{V}{n_\nu}\left|\Phi_j^\nu\right\rangle = \begin{cases} \sum_g D_{j'i'}^{\nu'*}(g) R(g) |\Phi_i^\nu\rangle, \text{ for finite groups,} \\ \int dg D_{j'i'}^{\nu'*}(g) R(g) |\Phi_i^\nu\rangle, \text{ for infinite groups} \end{cases}. \tag{2.23}$$

This leads to a natural definition of the operators

$$P_{ij}^\nu \equiv \frac{n_\nu}{V}\int dg D_{ij}^{\nu*}(g) R(g) \tag{2.24}$$

which means we can project out corresponding components

$$P_{ij}^\nu \left|\Phi_{j'}^{\nu'}\right\rangle = \delta_{\nu\nu'}\delta_{jj'} |\Phi_i^\nu\rangle \tag{2.25}$$

and they obey

$$P^{\nu}_{ij}P^{\nu'}_{i'j'} = \delta_{\nu\nu'}\delta_{ji'}P^{\nu}_{ij'}\ ,\ (P^{\nu}_{ij})^{\dagger} = P^{\nu}_{ij}. \tag{2.26}$$

For abelian groups we can define the projector that filters out the i-th columns of the ν-th irreducible representation as $P^{\nu}_{ii} = P^{\nu}_{i}$. These operators are both trivially hermitian and idempotent. For non-abelian groups however these operators give unphysical results as the action of the operators $P^{\nu}_{ii}\left|\Psi\right\rangle$ no longer gives the complete i-th column[6]. Therefore the (2.26) operator is needed to project out the correct representation in the irreducible subspace for non-abelian groups.

Following the reasoning in above the particle number projection operator can be seen as a one-dimensional rotation in gauge space[7],[4],[8]. Rotations along one-dimensions is abelian and with $g = \phi$ the symmetry operator is

$$R(\phi)\left|\Phi\right\rangle = e^{-i\phi\hat{N}}\left|\Phi\right\rangle, \tag{2.27}$$

in the representation $\nu = N$, $n_{\nu} = 1$ and thus, using (2.24);

$$\begin{aligned} V &= \int_0^{2\pi} d\phi = 2\pi, \\ D^N(\phi) &= e^{-iN\phi}, \\ P^N &\equiv \frac{1}{2\pi}\int d\phi e^{-i\phi(\hat{N}-N)}. \end{aligned} \tag{2.28}$$

This operator has a full resolution of unity as, with a complete and orthogonal set of Nilsson orbital configurations with good particle number $\left|N\right\rangle$ (neglecting the remaining good quantum numbers for convenience), we get

$$\begin{aligned} \mathbb{1}P^N\mathbb{1} = \sum_{N''}\left|N''\right\rangle\!\left\langle N''\right| \frac{1}{2\pi}\int d\phi e^{-i\phi(\hat{N}-N)}\sum_{N'}\left|N'\right\rangle\!\left\langle N'\right| = \\ \sum_{N',N''}\frac{1}{2\pi}\int d\phi e^{-i\phi(N'-N)}\left|N''\right\rangle\!\left\langle N''\right|\left|N'\right\rangle\!\left\langle N'\right| = \\ \sum_{N',N''}\delta_{N,N'}\delta_{N',N''}\left|N'\right\rangle\!\left\langle N''\right| = \sum_{N}\left|N\right\rangle\!\left\langle N\right| \end{aligned} \tag{2.29}$$

which spanns the whole set of single particle states. From (2.29) we can also see that P^N is truly a projection operator [9].

For the angular momentum projection the three-dimensional rotation group is usually parameterized by the Euler angles $g = \Omega = (\alpha, \beta, \gamma)$ and we use the angular momentum as the irreducible representation $\nu = I$, $n_{\nu} = 2I + 1$ which gives the group element and volume:

$$\begin{aligned} R(\Omega) &= e^{-i\alpha J_z}e^{-i\beta J_y}e^{-i\gamma J_z}, \\ V &= \int d\Omega = 8\pi^2. \end{aligned} \tag{2.30}$$

As mention above the irreducible representations are the Wigner D-functions, which do note commute as the group is non-abelian. If we use the generalised projector definition of (2.24) we get:

$$P^J_{MK} \equiv \frac{2J+1}{8\pi^2} \int d\Omega D^{J*}_{MK}(\Omega) R(\Omega), \tag{2.31}$$

which is, as mentioned, not a true projection operator. If we introduce a complete and orthogonal set of Nilsson orbital configurations with good quantum numbers of I^2 and I_z with the remaining good quantum numbers α denoted $|IM\alpha\rangle$ we see that

$$R(\Omega) \left|JM\alpha\right\rangle = \sum_K D^J_{KM}(\Omega) \left|JK\alpha\right\rangle . \tag{2.32}$$

So expanding the operator (2.31) (again, using ... to denote line break);

$$\begin{aligned}
\mathbb{1} P^J_{MK} \mathbb{1} = \sum_{J'M''\alpha} |J'M''\alpha\rangle\langle J'M''\alpha| \frac{2J+1}{8\pi^2} \int d\Omega D^{J*}_{MK}(\Omega) R(\Omega) \cdot \ldots \\
\ldots \cdot \sum_{I'M'\alpha} |I'M'\alpha\rangle\langle I'M'\alpha| = \\
\frac{2J+1}{8\pi^2} \sum_{J'M''M'K\alpha} |J'M''\alpha\rangle\langle J'M''\alpha| \cdot \ldots \\
\ldots \cdot \left(\int d\Omega D^{I*}_{MK} D^{J'}_{K'M'}(\Omega) \right) |J'K'\alpha\rangle \langle J'M'\alpha| = \\
\sum_{M''\alpha} |JM''\alpha\rangle \langle JM''\alpha|JM\alpha\rangle \langle JK\alpha| = \sum_\alpha |JM\alpha\rangle\langle JK\alpha|
\end{aligned} \tag{2.33}$$

which clearly does not completely resolve unity. As mentioned above, even the diagonal form of P^J_{MM} can't be used, which we now clearly see from (2.33) as would only project out the M-th state, when in fact all states with $K = M \in \{-I, -I+1, \ldots, I\}$ are needed to span the J-th irreducible subspace. To find the complete representation we thus need to expand the projection operator in the K-th columns as [4],[7]:

$$\left|\Psi^J_K\right\rangle = \sum_K g_K P^J_{MK} \left|\Phi\right\rangle = \sum_K \frac{2J+1}{8\pi^2} \int d\Omega g_k D^{J*}_{MK}(\Omega) R(\Omega) \left|\Phi\right\rangle . \tag{2.34}$$

where $\left|\Psi^J_K\right\rangle$ is a many-body state with good quantum numbers

$$J^2 \left|\Psi^J_K\right\rangle = J(J+1) \left|\Psi^I_K\right\rangle \text{ and } J_z \left|\Psi^J_K\right\rangle = M \left|\Psi^J_K\right\rangle , \tag{2.35}$$

as can be seen from the derivation (2.33). However we've now introduced a new unknown into the problem, the expansion coefficients g_K, which needs to be determined. To do so we use the so-called generator coordinate method to minimize the projected energy with respect to these coefficients.

2.3 Generator Coordinate Method

To describe collective phenomena of nuclei such as collective motion, deformation and rotation but also pairing correlations between nucleons it is common to employ the generator coordinate method (GCM). The minimization of the projected wave function is in itself only a special case of the GCM method. The state of the nuclei $|\Psi\rangle$ is assumed to be a continuous sum of coherent collective wave-functions along a path of generator coordinates $\{a\}$, that is[4]:

$$|\Psi\rangle = \int da f(a) \, |\phi(a)\rangle \, . \tag{2.36}$$

The function $f(a)$ is called the generator function, which acts as a weight depending on the continuous summation index a. When minimizing the projected states, the summation index is the group elements and the weight functions are the irreducible matrix representations $D^{\nu'}_{j'i'}(g)$. In general the generator coordinates are multidimensional complex parameters chosen to fit the potential of interest. In the DFT to effective Hamiltonian calculations a (γ, β_2) quadrupole deformation parameter expansion is used. For the restoration of symmetries we should then add to the generator coordinates the Euler angles $\Omega = (\alpha, \beta, \gamma)$ and the gauge angle in neutron and proton number φ_N, φ_Z. The total set of generator coordinates used would be $a = (\gamma, \beta_2, \Omega, \varphi_N, \varphi_Z)$, however time constraint left us with only $a = (\gamma, \beta_2, \varphi_N, \varphi_Z)$.

To determine a good approximation of the symmetry preserving ground state of the nuclei, we need to determine the minimum of the energy functional

$$E\{\phi(a)\} \equiv \frac{\langle \Psi | H | \Psi \rangle}{\langle \Psi | \Psi \rangle}, \tag{2.37}$$

this energy functional is a multidimensional surface which depends upon the generator coordinates used. It can be minimized with respect to the weight functions, which stand to be determined for the continuous expansion:

$$\frac{\delta E\{\phi(a)\}}{\delta f(a)} = 0. \tag{2.38}$$

In accordance with [10], [11] this minimization is then formulated as an integral equation, the so called Hill-Wheeler equation:

$$\begin{gathered} \int db \, [\mathscr{H}(a,b) - E\mathscr{O}(a,b)] \, f(b) = 0 \\ \mathscr{H}(a,b) \equiv \langle \phi(a) | H | \phi(b) \rangle \quad , \quad \mathscr{O}(a,b) \equiv \langle \phi(a) | \phi(b) \rangle \, . \end{gathered} \tag{2.39}$$

A more general form of this equation is:

$$\mathscr{H} f = E \mathscr{O} f. \tag{2.40}$$

Constructing a combined symmetry operator for the angular momentum J using (2.34) and neutron and proton number Z, N from (2.28), we get

$$P^{JM}_{N,Z} \equiv \sum_K g_K P^J_{MK} P^N P^Z = \sum_K g_K P^{J,MK}_{N,Z}. \tag{2.41}$$

Denoting the the symmetry conserving state $\left|\Psi^{J,M}_{N,Z}\right\rangle$ we arrive at the equation [4],[12]:

$$E^P = \frac{\left\langle \Psi^{J,M}_{N,Z} \middle| H \middle| \Psi^{J,M}_{N,Z} \right\rangle}{\left\langle \Psi^{J,M}_{N,Z} \middle| \Psi^{J,M}_{N,Z} \right\rangle} = \frac{\sum_{KK'} g^*_K g_{K'} h^J_{KK'}}{\sum_{KK'} g^*_K g_{K'} n^J_{KK'}}, \tag{2.42}$$

with the projected kernels, using the fact that the projector is idempotent and commutes with the Hamiltonian,

$$\begin{aligned} h^J_{KK'} &= \langle \Phi | H P^{J,KK'}_{N,Z} | \Phi \rangle \,, \\ n^J_{KK'} &= \langle \Phi | P^{J,KK'}_{N,Z} | \Phi \rangle \,. \end{aligned} \tag{2.43}$$

The coefficients g_K are then to be determined by the eigenvalue problem[4]

$$\sum_{K'} h^J_{KK'} g_{K'} = E^P \sum_{K'} n^J_{KK'} g_{K'}. \tag{2.44}$$

This result is a matrix equation of the form (2.40). How to solve this equation is a topic beyond the scope of this thesis, but it is done for the DFT to Hamiltonian calculations. The focus of this thesis is instead on how to calculate the actual matrix elements of equation (2.43).

2.4 Projected matrix elements

For all of the symmetry transformations $R(g)$ introduced above the generators are one-body Hermitian operators G, which can be written as [13]:

$$R = e^{iG}. \tag{2.45}$$

From this we can define the transformation in the HFB formalism, starting from the single particle orbitals, using the creation and annihilation operators[14]

$$R c^\dagger_i R^\dagger = \sum_j R_{ij} c^\dagger_j \,, \; R c_i R^\dagger = \sum_j R^*_{ij} c^\dagger_j, \tag{2.46}$$

where each, letting Ω denote the three-dimensional Euler angles,

$$R_{ij} = R_{ij}(\Omega, N, Z) = \langle i | \, e^{-i\alpha J_z} e^{-i\beta J_y} e^{-i\gamma J_z} e^{-i\phi_N \hat{N}} e^{-i\phi_Z \hat{Z}} \, | j \rangle \,. \tag{2.47}$$

Where R_{ij} is the matrix elements of the operator in the single-particle Nilsson orbitals. This can be cast in matrix form as [15], with $\Theta \equiv (\Omega, N, Z)$ and $R(\Theta) = R_\Theta$;

$$R_\Theta \begin{pmatrix} c^\dagger \\ c \end{pmatrix} R_\Theta^\dagger = \begin{pmatrix} R_\Theta^T & 0 \\ 0 & R_\Theta^\dagger \end{pmatrix} \begin{pmatrix} c^\dagger \\ c \end{pmatrix} \equiv \begin{pmatrix} \tilde{c}^\dagger \\ \tilde{c} \end{pmatrix}. \tag{2.48}$$

From the quasi-particle transformation we can define a new, rotated quasi-particle vacuum:

$$\begin{pmatrix} \tilde{b} \\ \tilde{b}^\dagger \end{pmatrix} = \mathcal{W}^\dagger \begin{pmatrix} \tilde{c}^\dagger \\ \tilde{c} \end{pmatrix} = \begin{pmatrix} [R_\Theta^\dagger U]^\dagger & [R_\Theta^* V]^\dagger \\ [R_\Theta^* V]^T & [R_\Theta U]^T \end{pmatrix} \begin{pmatrix} c^\dagger \\ c \end{pmatrix} \equiv \tilde{\mathcal{W}}^\dagger(\Theta) \begin{pmatrix} c^\dagger \\ c \end{pmatrix}. \tag{2.49}$$

Which means a quasi-particle vacuum $|\Phi\rangle$ and its rotated analog $R_\Theta |\Phi\rangle \equiv |\Phi_\Theta\rangle$ can be expressed in the following matrix form:

$$\begin{aligned} |\Phi\rangle &\shortmid\longrightarrow \begin{pmatrix} b \\ b^\dagger \end{pmatrix} = \mathcal{W}^\dagger \begin{pmatrix} c^\dagger \\ c \end{pmatrix}, \\ |\Phi_\Theta\rangle &\shortmid\longrightarrow \begin{pmatrix} \tilde{b} \\ \tilde{b}^\dagger \end{pmatrix} = \mathcal{W}^\dagger(\Theta) \begin{pmatrix} c^\dagger \\ c \end{pmatrix}. \end{aligned} \tag{2.50}$$

The norm kernel can now be written as:

$$\begin{aligned} \langle \Phi | P_{N,Z}^{J,KK'} | \Phi' \rangle = \frac{2I+1}{32\pi^4} \int d\Omega D_{KK'}^{J*}(\Omega) \int d\varphi_N e^{i\varphi N} \int d\phi_Z e^{i\varphi N} \cdot \ldots \\ \ldots \cdot \langle \Phi | R_{d\Theta} | \Phi' \rangle \equiv \mathscr{I}_{d\Theta} \langle \Phi | \Phi'_{d\Theta} \rangle. \end{aligned} \tag{2.51}$$

Equation (2.51) introduce the main computational problem of investigation in this thesis; integration and the evaluate of the overlap at each point of integration. To evaluate the integrals on a computer some sort of discretization is needed. One way of doing this is following [16],[8] and using a straight forward (left) Riemann sum. For the particle number (both proton and neutron numbers), with the mesh divided into L points, we get

$$\frac{1}{2\pi} \int_0^{2\pi} d\varphi e^{-i\varphi(\hat{N}-N)} \longrightarrow \frac{1}{2\pi} \sum_{k=0}^{L} \Delta\varphi e^{-i\Delta\varphi \cdot k(\hat{N}-N)} \quad , \Delta\varphi = \frac{2\pi}{L+1} \tag{2.52}$$

whereas for the angular momentum projection, starting by using the definition of the Wigner D-functions

$$\begin{aligned} \frac{2J+1}{8\pi^2} \int d\Omega D_{MK}^{J*}(\Omega) = \frac{1}{2\pi} \int_0^{2\pi} d\gamma e^{-i\gamma M} \frac{1}{2\pi} \int_0^{2\pi} d\alpha e^{-i\alpha K} \cdot \ldots \\ \ldots \cdot \frac{2J+1}{2} \int_0^{\pi} d\beta \, \sin(\beta) \, d_{MK}^{J*}(\beta) \, e^{-iJ_y\beta}. \end{aligned} \tag{2.53}$$

The first two integrals of (2.53) and (2.52) being very similar leads us to a totally analogous discretization of both. For the third and last integral of (2.53),

which now contains the Wigner small d-matrix, the following left Riemann sum discretization is made;

$$\int_0^\pi d\beta \sin(\beta) d^{J*}_{MK}(\beta) e^{-iJ_y\beta} \longrightarrow \sum_{k=0}^{L} \Delta\beta \sin(\Delta\beta \cdot k) e^{-i\Delta\beta\cdot k J_y} d^{J*}_{MK}(\Delta\beta\cdot k) \ \ , \Delta\beta = \frac{\pi}{L+1}. \tag{2.54}$$

What remains now for the norm kernel is the overlap $\langle\Phi|\Phi_{\delta\Theta}\rangle$, whose arguments are now discretized as well which is denote by the δ. It turns out that this problem is also the core computational challenge of the Hamiltonian kernel. Using Thouless' theorem together with Wick's theorem, one can show that [4],[7]:

$$\begin{aligned} h^J_{KK'} = \ & \langle\Phi|HP^{J,KK'}_{N,Z}|\Phi'\rangle = \mathscr{I}_{\delta\Theta}\langle\Phi|H|\Phi'_{\delta\Theta}\rangle = \\ & \mathscr{I}_{\delta\Theta}\langle\Phi|\Phi'_{\delta\Theta}\rangle \left\{ \mathrm{Tr}(\varepsilon\rho(\delta\Theta)) + \frac{1}{2}\mathrm{Tr}(\Gamma(\delta\Theta)\rho(\delta\Theta)) - \frac{1}{2}\mathrm{Tr}(\Delta(\delta\Theta)\bar{\kappa}^*(\delta\Theta)) \right\}, \end{aligned} \tag{2.55}$$

where ε is the single particle energy and the one body transition density matrix ρ and pairing tensors $\kappa, \bar{\kappa}^*$:

$$\begin{aligned} \mathbb{U}_{\delta\Theta} &\equiv U'^{\dagger} R^{\dagger}_{\delta\Theta} U + V'^{\dagger} R^{T}_{\delta\Theta} V, \\ \rho_{nn'}(\delta\Theta) &= \langle\Phi|c^{\dagger}_{n'}c_n|\Phi'_{\delta\Theta}\rangle = (R_{\delta\Theta}V'^{*}\mathbb{U}^{T^{-1}}_{\delta\Theta}V^T)_{nn'}, \\ \kappa_{nn'}(\delta\Theta) &= \langle\Phi|c_{n'}c_n|\Phi'_{\delta\Theta}\rangle = (R_{\delta\Theta}V'^{*}\mathbb{U}^{T^{-1}}_{\delta\Theta}U^T)_{nn'} \\ \bar{\kappa}^*_{nn'}(\delta\Theta) &= \langle\Phi|c^{\dagger}_n c^{\dagger}_{n'}|\Phi'_{\delta\Theta}\rangle = -(R_{\delta\Theta}U'^{*}\mathbb{U}^{T^{-1}}_{\delta\Theta}U^T)_{nn'}. \end{aligned} \tag{2.56}$$

using the rotated fields $\Gamma(\delta\Theta), \Delta(\delta\Theta)$ defined using matrix multiplications as;

$$\begin{aligned} \Gamma_{nm}(\delta\Theta) &= \sum_{n'm'} v_{nn'mm'}\rho_{m'n'}(\delta\Theta) = \sum_{n'm'} G\rho_{m'n'}(\delta\Theta), \\ \Delta_{nm}(\delta\Theta) &= \frac{1}{2}\sum_{m'n'} v_{nmn'm'}\kappa_{n'm'}(\delta\Theta) = \frac{1}{2}\sum_{n'm'} G\rho_{m'n'}(\delta\Theta). \end{aligned} \tag{2.57}$$

Yet again, what remains to be found is thus the overlap in (2.55). This can be done either using the Onishi formula or the Pfaffian [17],[7]. The Onishi formula makes for a rather straight forward computation, but leaves the phase of the overlap undefined. The main part of the computational focus of this thesis is the Pfaffian approach.

2.5 The Pfaffian

To calculate the overlap between different and rotated quasi-particle vacuums three different algortihms were used and tested for performance. The main focus of this thesis is the Pfaffian approach, the derivation of which is can be done in many

different ways [14],[4],[18],[19] but is outside of this thesis. The results gives that, for two normalized states [14]:

$$\langle\Phi|\Phi'_{\delta\Theta}\rangle = \frac{(-1)^{n(n-1)/2}}{\prod_\alpha^n V_\alpha V'_\alpha}\mathrm{Pf}\begin{bmatrix} V^TU & V^TR^T_{\delta\Theta}V'^* \\ -V'^\dagger R_{\delta\Theta}V' & U'^\dagger V^* \end{bmatrix} = \frac{S_n}{\mathcal{N}\mathcal{N}'}\mathrm{Pf}[\mathcal{M}_{\delta\Theta}], \quad (2.58)$$

with

$$\mathcal{M}_{\delta\Theta} \equiv \begin{pmatrix} V^TU & V^TR^T_{\delta\Theta}V'^* \\ -V'^\dagger R_{\delta\Theta}V' & U'^\dagger V^* \end{pmatrix}, \quad (2.59)$$

and $S_n \equiv (-1)^{n(n-1)/2}$ is the overall phase after normal ordering and the norm $\mathcal{N}$ is calculated as

$$\mathcal{N} \equiv \langle\Phi|\Phi\rangle = (-1)^n\mathrm{Pf}\begin{bmatrix} V^TU & V^TV^* \\ -V^\dagger V & U^\dagger V^* \end{bmatrix} = (-1)^n\mathrm{Pf}[\mathcal{M}] = \prod_\alpha^n V_\alpha^2. \quad (2.60)$$

For comparison, the Onishi formula is defined as, with the definition of (2.57) [12]:

$$\langle\Phi|\Phi'_{\delta\Theta}\rangle^2 = \mathrm{Det}[\mathbb{U}_{\delta\Theta}]. \quad (2.61)$$

The Pfaffian itself is intimately connected to the determinant, as can be seen from the combination of (2.58) and (2.61). The Pfaffian is defined only for a skew-symmetric matrix $A : A \in \mathbb{C}^{2n\times 2n}$, where skew-symmetric means that $A = -A^T$. For such matrix the determinant is the square of a polynomial of degree n called the Pfaffian, thus the Pfaffian is a unique choice for the square root of the determinant:

$$\mathrm{Pf}(A) = \sqrt{\mathrm{Det}(A)}. \quad (2.62)$$

The most general definiton of the Pfaffian is given by the equation [2],[1]:

$$\mathrm{Pf}(A) = \frac{1}{2^n n!}\sum_{\sigma\in S_{2n}}\mathrm{sgn}(\sigma)\prod_i^n a_{\sigma(2i-1),\sigma(2i)} \quad (2.63)$$

with S_{2n} being the group of permutations of sets with $2n$ elements and $\mathrm{sgn}(\sigma)$ is the signature of σ. By definition, the Pfaffian of an odd-dimensional matrix is zero, as the determinant of a an odd skew-symmetric is zero.

The computational cost of definition (2.63) being of $\mathcal{O}(n!)$ means it does not lend it self to implementation on larger model spaces or realistic physical calculations. To find a more computationally feasible implementation the recursive definition of the Pfaffian is used [2]:

$$\mathrm{Pf}(A) = \sum_{i=2}^{2n}(-1)^i\mathrm{Pf}(A_{1i}). \quad (2.64)$$

where A_{1i} is the matrix A without row 1 and column i. From this definition it is

evident that for a tridiagonal matrix A_T the Pfaffian is particularly simple;

$$\mathrm{Pf}(A_T) = \mathrm{Pf}\begin{bmatrix} 0 & a_1 & & & & & \\ -a_1 & 0 & b_1 & & & & \\ & -b_1 & 0 & a_2 & & & \\ & & -a_2 & \ddots & \ddots & & \\ & & & \ddots & \ddots & b_{n-1} & \\ & & & & -b_{n-1} & 0 & a_n \\ & & & & & -a_n & 0 \end{bmatrix} = \prod_{i=1}^{n} a_n. \tag{2.65}$$

But also for an *almost* triadiagonal matrix $A_{\tilde{T}}$, a matrix for which the removal of the odd rows would yield a tridiagonal matrix, the result is the same as in (2.65);

$$\mathrm{Pf}(A_{\tilde{T}}) = \mathrm{Pf}\begin{bmatrix} 0 & a_1 & & & & & \\ -a_1 & 0 & c_{23} & c_{24} & c_{25} & \dots & \\ & -c_{23} & 0 & a_2 & & & \\ & -c_{24} & -a_2 & \ddots & \ddots & & \\ & -c_{25} & & \ddots & \ddots & c_{2n-1,2n-1} & c_{2n-1,2n} \\ & \vdots & & & -c_{2n-1,2n-1} & 0 & a_n \\ & & & & -c_{2n-1,2n} & -a_n & 0 \end{bmatrix} = \prod_{i=1}^{n} a_n. \tag{2.66}$$

At the same time the, for an arbitrary matrix B : $B \in \mathbb{C}^{2n\times 2n}$ one can construct a transformation BAB^T for which

$$\mathrm{Pf}(BAB^T) = \mathrm{Det}(B)\mathrm{Pf}(A) \tag{2.67}$$

As such calculating the Pfaffian of A can be greatly simplified by finding a (invertible) transformation matrix B that brings the A to tridiagonal form.

Chapter 3

Results and Discussion

3.1 Particle number projection

Here the results of particle number projection in the BCS with seniority pairing-model, using a total of $N = 5$ principal Nilsson shells, are presented. Adding the mean-field pairing interaction to the Nilsson oscillator scatters the nucleons around the fermi level while breaking particle number symmetry. This results in a change of the occupation of the single-particle orbitals, giving tails in the V_α, U_α coefficients into previously unoccupied states, but also spreads the many-body state in particle number (N/Z) space. The calculations are made for ${}^{18}_{8}\mathrm{O}$ and ${}^{48}_{24}\mathrm{Cr}$ using the empirical relationship for the pairing interaction (2.16). The particle number projection is calculated as, using definitions from (2.58) and (2.52);

$$\begin{aligned} P_{[N]} &:= \frac{\langle\Phi|P_N|\Phi\rangle}{\langle\Phi|\Phi\rangle} = \frac{1}{2\pi}\sum_{k=0}^{L}\Delta\varphi\, e^{i\Delta\varphi kN}\,\mathrm{Pf}[\mathcal{M}_{\delta\Theta}], \\ P_{[Z]} &:= \frac{\langle\Phi|P_Z|\Phi\rangle}{\langle\Phi|\Phi\rangle} = \frac{1}{2\pi}\sum_{k=0}^{L}\Delta\varphi\, e^{i\Delta\varphi kZ}\,\mathrm{Pf}[\mathcal{M}_{\delta\Theta}], \\ &\delta\Theta = \Delta\varphi, \end{aligned} \tag{3.1}$$

using $L = 16$ to guarantee convergence and the method of Householder reflections for complex matrices from [2] to reduce runtime of calculations (see next section for Pfaffian performance analysis).

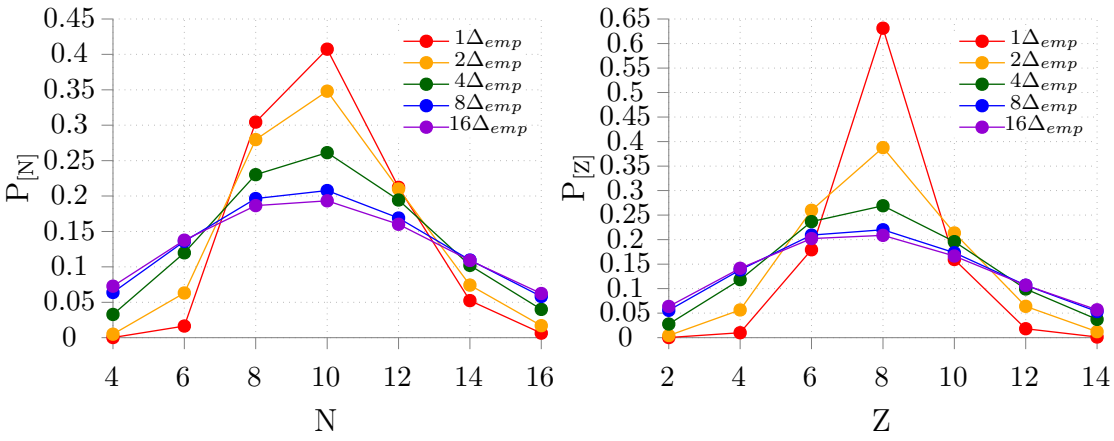

(a) Neutrons: $\hbar\omega_0 = 16.22$ MeV

(b) Protons: $\hbar\omega_0 = 15.07$ MeV

Figure 3.1: Amplitude of the particle number operator (3.1) for neutrons (N) and protons (Z) in $^{18}_{8}$O.

$i \cdot \Delta_{emp}$ [N/A]	Energy [MeV]
1	2.88
2	5.66
4	11.31
8	22.63
16	45.25

Table 3.1: Multiples, i, of the empirical pairing gap in MeV for $^{18}_{8}$O.

In figure 3.1 the amplitude of the particle number projection for neutrons and protons are plotted using a pairing gap in multiples, i, of Δ_{emp}, see table 3.1 for numerical values. One can clearly see that for the protons, with only the empirical pairing, being magic in number gives a large peak in particle number for exactly this number of protons. The distribution then subsides quickly on either end of $Z = 8$. For increasing multiples of the pairing strength the distribution of proton number spreads more and more into other states of even proton numbers, the peak around $Z = 8$ becoming less and less prominent. For the neutron number on the other hand, using the empirical gap, the neutron number is clearly peaked for $N = 10$ however not as much nor as sharp as for the protons. This is to be expected as the pairing interaction is greater for non-magic i.e. non-closed and tightly bound shells. In a similar manner to the protons, the neutron number gets a less pronounced peak and gets more evenly distributed among even numbered states for increasing multiples of pairing gap. Moreover one can see that as the pairing gap becomes of similar order as the oscillator frequency, which happens for $4 \cdot \Delta_{emp}$ for both protons and neutrons (see table 3.1) the pairing interaction is so strong that it completely dictates the distribution of particle number. This causes both of the distributions to look almost completely the same for the larger pairing gaps.

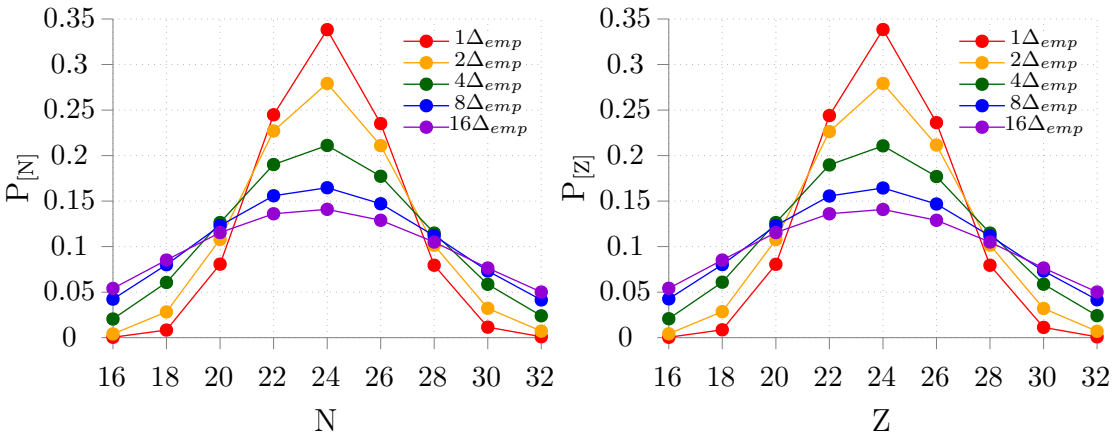

(a) Neutrons: $\hbar\omega_0 = 11.28$ MeV (b) Protons: $\hbar\omega_0 = 11.28$ MeV

Figure 3.2: Amplitude of the particle number operator (3.1) for neutrons and protons on $^{48}_{24}$Cr.

$i \cdot \Delta_{emp}$ [N/A]	Energy [MeV]
1	1.73
2	3.46
4	6.92
8	13.86
16	27.71

Table 3.2: Multiples, i, of the empirical pairing gap in MeV for $^{48}_{24}$Cr.

In figure 3.2 the amplitude of the particle number projection for the N=Z nucleus $^{48}_{24}$Cr is presented, with the strength of the multiples, i, of the empirical pairing gap given in table 3.2. The distribution for both proton and neutron number look very similar, which they should as the oscillator frequency for both nucleons is the same up to two significant figures. Similar to the case for oxygen-18, as the pairing gap becomes in the order of $\hbar\omega_0$, which is the case for $i = 4$ for chromium-48, the pairing gap dominates the oscillator potential and thus also the particle number distribution.

3.2 Pfaffian performance

In this section the results of the performance test of different Pfaffian routines of [2] and [1], using the different algorithms outlined in the section above, is presented. From the work in [2] the Parlett-Reid and Householder routines are used, whereas from [1] a routine using the algorithm of Atiken is employed.

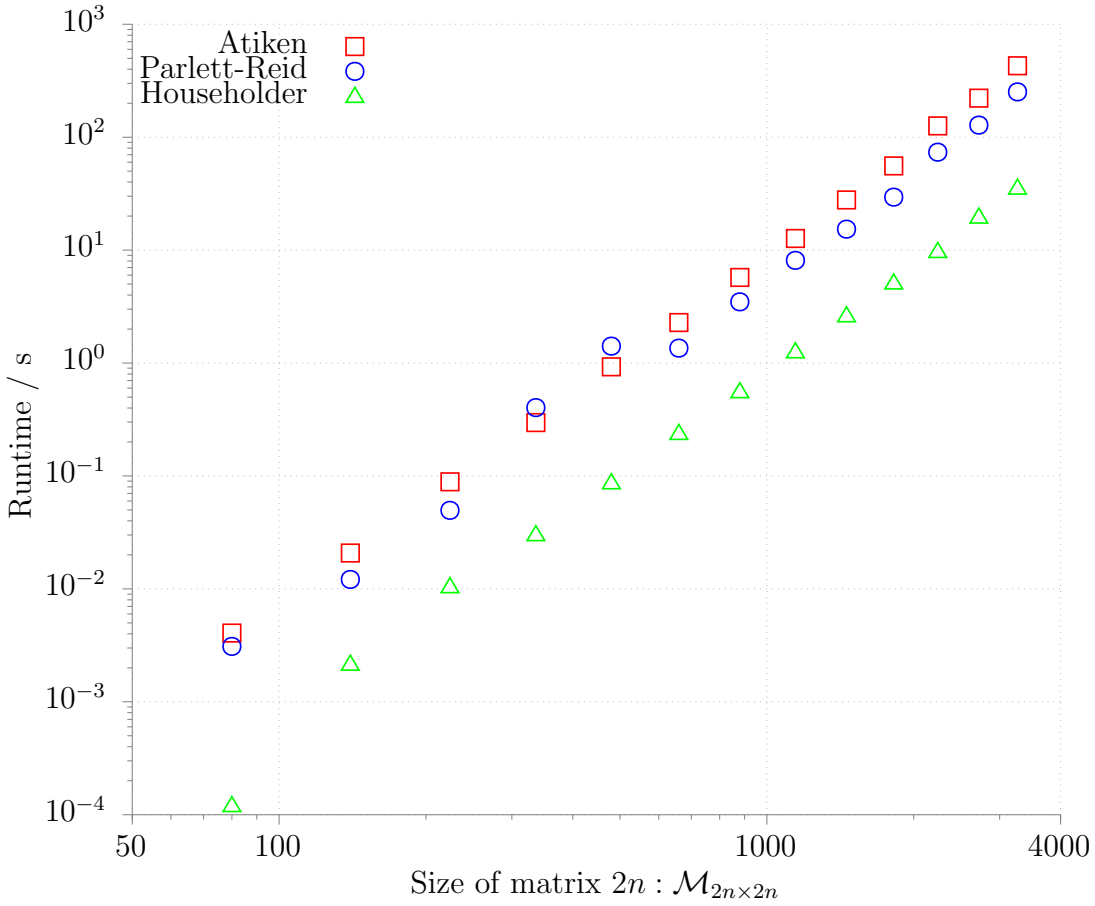

Figure 3.3: The run-time of the Pfaffian routines.

The seniority pairing-model, using a HFB-formalism outlined in the previous sections, is used to calculate the norm $\langle\Phi|\Phi\rangle = \mathcal{N}$ of the ground state of $^{48}_{24}$Cr using (2.60):

$$\mathcal{N} = (-1)^n \mathrm{Pf}\begin{bmatrix} V^T U & V^T V^* \\ -V^\dagger V & U^\dagger V^* \end{bmatrix} = (-1)^n \mathrm{Pf}[\mathcal{M}]$$

The principal quantum number N_{osc}, whose degeneracy is $\sum_{N'=1}^{N_{osc}}(N'+1)(N'+2)$, is allowed to vary from $N_{osc} = 3$ to $N_{osc} = 15$. This gives a model spaces of n = 38 up to n = 1630 independent levels, one set for protons and neutrons each. In figure 3.3 above, the runtime of the different Pfaffian routines for the different sized model spaces are plotted. Clearly the routine of [2] using the Householder

reflections is the fastest throughout. Both the Parlett-Reid and the Atiken routines fair so similar that no preference can really be had.

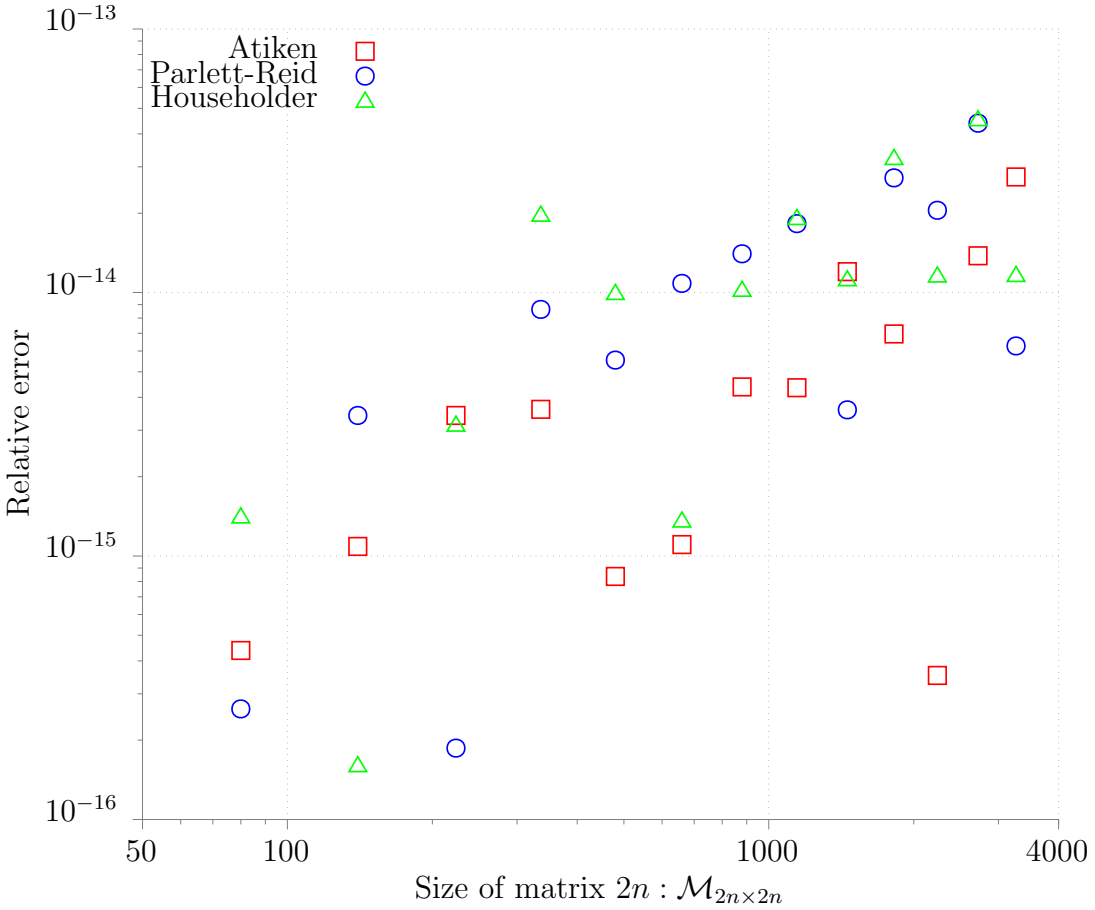

Figure 3.4: The relative error (3.2) of the Pfaffian routines.

In figure 3.4 above the relative error of the routines as the models pace varies in size is plotted. The relative error of the overlaps are calculated using (2.60), noting the fact that the Pfaffian should equal the product of the V_α^2:

$$\text{Relative error} := \left| \frac{\prod_\alpha^n V_\alpha^2 - \mathcal{N}}{\prod_\alpha^n V_\alpha^2} \right|. \tag{3.2}$$

It can be seen that on average the Atiken routine of [1] is the least erroneous, while for the two routines of [2] are more or less performing equally. However the errors for all of the routines are so small that for implementations on physical systems, with a total number of principal shells between $20 - 50$ [20],[3], the difference in runtime should be much more of a determining factor. As such, the routine of [2] implementing Householder reflections is to be preferred when making future calculations.

3.3 Model space truncation

This section presents the results of the investigation into the particle number stability of a truncated model space. Two different methods of truncation was used: one method modifies the U_α, V_α factors when they pass below a certain threshold value ε by simply replacing them with ε as $U_\alpha^2 < \varepsilon$ or $V_\alpha^2 < \varepsilon$. The other method properly truncates the HFB-wave function $\mathcal{W}$ by removing the rows and columns of the constituting U, V-matrices for states α such that $V_\alpha^2 < \gamma$. From here on the former method will be called the ε-method and the latter will be referred to as the γ-method.

The stability of the methods is evaluated using the expectation value of the neutron number calculated as

$$\langle N \rangle = \frac{\langle \Phi | N P_N | \Phi \rangle}{\langle \Phi | P_N | \Phi \rangle} = \frac{\mathscr{J}_{d\Theta} \langle \Phi | \Phi_{\delta\Theta} \rangle \cdot \mathrm{Tr} \left[R_{\delta\Theta} V^* \mathbb{U}_{\delta\Theta}^{T^{-1}} V^T \right]}{\mathscr{J}_{d\Theta'} \langle \Phi | \Phi_{\delta\Theta'} \rangle}, \tag{3.3}$$

for the $^{48}_{24}$Cr nucleus used previously, with a pairing gap of Δ_{emp} (see table 3.2). The size of the model space is varied between $N_{osc} = 5, \ldots, 13$ giving set of single particle levels between n= 110 up to n= 1118. The expectation value is calculated for $N = 18, \ldots, 30$ and when $|\langle N \rangle - N| > 10^{-2}$ the method is deemed unstable.

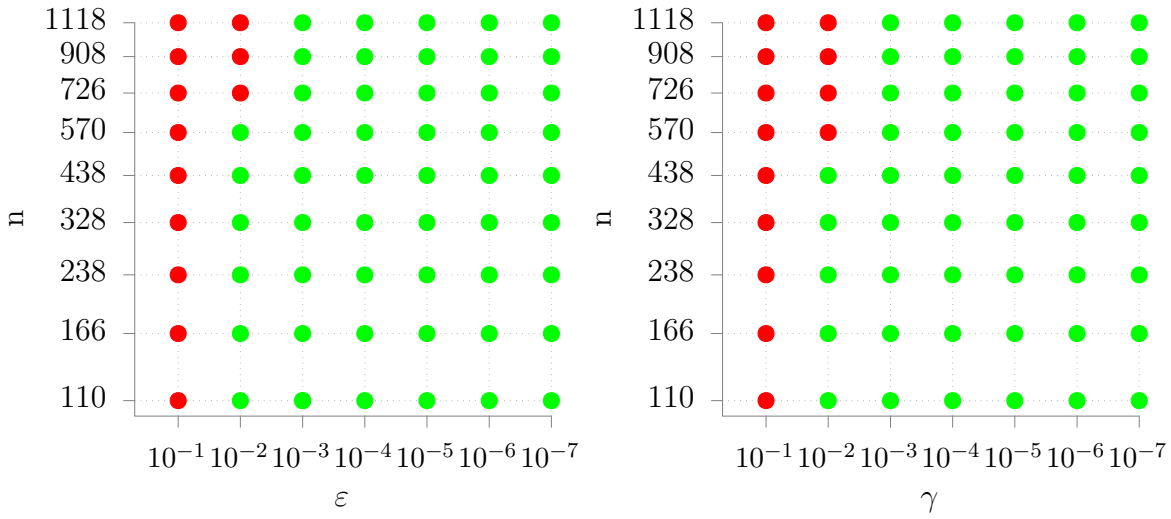

Figure 3.5: A classification plot of the ε and γ-method, calculated for $^{48}_{24}$Cr. The green dot signifies a stable calculation of $\langle N \rangle$, while a red dot signifies a non-stable result.

One expects that the U_α^2, V_α^2 should reach lower values for larger model spaces because as they both vary between 1 to 0, a larger model space gives a higher resolution of the interval meaning that larger n gives more values close to 0 . Hence it can be reasoned that larger model spaces will be more affected by truncation, giving some n dependency on the stability of the methods.

As can be seen in figure 3.5 both the methods are stable for values of ε, γ below 10^{-2}. The reason for this could be due to the fact that the U_α^2, V_α^2 never reach values low enough for the truncation to take effect or that the influence of the truncation preserve stability. This test is unfortunately inconclusive here. Both methods also break down for $\varepsilon, \gamma = 10^{-2}$, but for different n - as was argued for above. This gives a weak implication that the ε-method is a the more stable method, probably due to the fact that it does not actually remove contributions to the U_α^2, V_α^2 but instead forces them to stay above the threshold.

It is impossible to make a conclusive analysis of the methods using the data at hand. Further investigations with larger model spaces would be needed before making a judgment. The purpose of the truncation is to decrease runtime at a reasonable cost of stability - this is much valued pursuit and worth undertaking. The γ, ε range is likely decent, as smaller values of ε, γ would probably yield more stable results for larger model spaces, but would likely also defeat the purpose of the truncation. See the conclusion and outlook section for further suggestions.

3.4 Symmetry restoration in post-DFT calculations

In this section the results of implementing particle number restoration in a post-DFT calculation for ${}^{18}_{8}\mathrm{O}$ are presented. The code used in the previous sections are implemented inside an extension of the *HOSHPE*[3] program which uses a spherical harmonic oscillator basis as input for Skyrme SLy4 [21] calculations of energy density functionals. These energies were then used to fit an effective-force, pairing plus quadrupole Hamiltonian to be used in Hartree-Fock-Bogoliubov calculations of differently deformed states in the (β, γ)-plane. Using these symmetry violating slater determinants in a variation after projection configuration mixing calculation with (β, γ, Z, N) as generator coordinates the ground state was approximated.

The Skyrme interaction is a phenomenologically motivated density dependent effective interaction. The force can be derived from the Hartree-Fock expectation value of a zero-range momentum-dependent two body force, first introduced by Skyrme in 1956 [4]. The force is expressed as a sum of different terms pertaining to: a central interaction, non-local interactions, density-dependent forces and a spin-orbit interaction. In the SLy4 parametrisation the pairing-interaction from the energy functional is dropped while using a separate density for neutrons and protons. This approach introduces a total of 10 terms that are fitted to nuclear structure data, see [22], [21] for further reference.

The deformation parameters γ, β in the plots are defined using the Lund convention; rotating the classical β-plane by 30°. The classical definition of the Hill-

Wheeler parameter gives β as, using spherical harmonics $Y_{\ell m}$,

$$\beta = \sqrt{\beta_x^2 + \beta_y^2}, \quad \text{with} \quad \beta_x = \frac{\sqrt{4\pi}}{5}\frac{\langle r^2 Y_{20}\rangle}{\langle r^2 Y_{00}\rangle}, \quad \beta_y = \frac{\sqrt{8\pi}}{5}\frac{\langle r^2 Y_{22}\rangle}{\langle r^2 Y_{00}\rangle}. \tag{3.4}$$

Rotating the the coordinate-space by 30° then gives

$$\begin{aligned} \beta_x &\to \beta \cdot \cos\left(\theta + \frac{30}{360}2\pi\right), \\ \beta_y &\to \beta \cdot \sin\left(\theta + \frac{30}{360}2\pi\right). \end{aligned} \tag{3.5}$$

From this β one then defines $\gamma = \operatorname{atan}\left(\frac{\beta_y}{\beta_x}\right)$. Only the $\gamma = 0°$ to $60°$ is plotted as it contains all possible deformations, the other sections only represent different rotational aligment. The $(0, 0)$ point represent sphericity. Along the $\gamma = 0°$ axis the deformation goes from spherical to prolate and along the axis of $\gamma = 60°$ the nuclei goes towards oblate from origo.

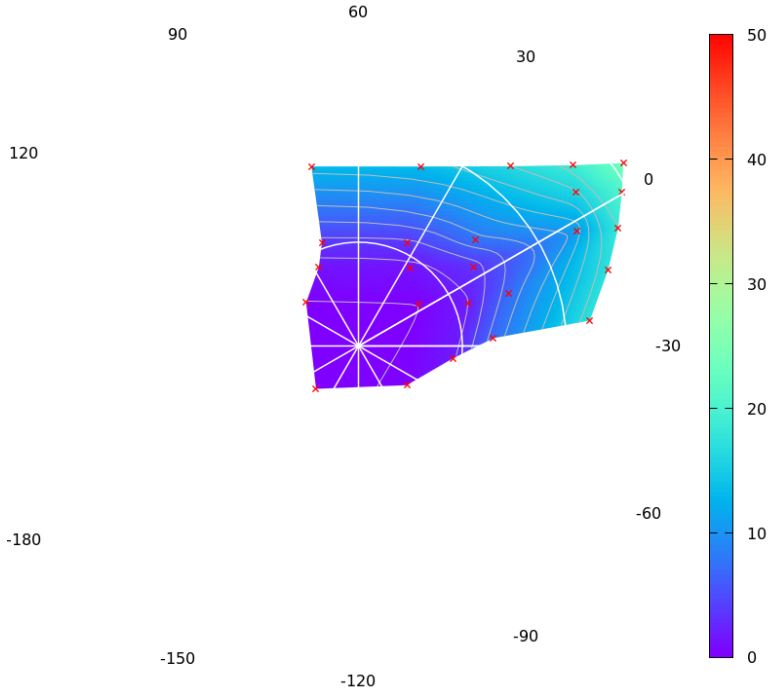

Figure 3.6: The energy surface of the HFB-calculation in the (β, γ)-plane.

In figure 3.6 is the energy surface of the unprojected HFB states calculated at different lattice points of triaxial γ and quadrupole β deformation. The energy surface shows a clear minimum for spherical deformation for the oxygen-18 nucleus.

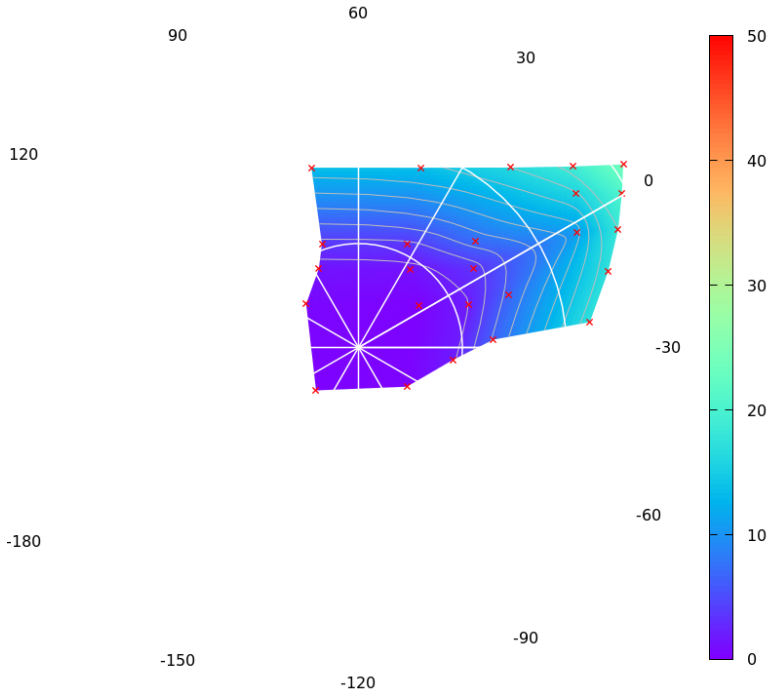

Figure 3.7: The 'projected' energy surface of the generator coordinate mixing.

In figure 3.7 the result of applying configuration mixing using deformation, neutron and proton numbers is presented. Using the different lattice states $|\phi\rangle$ pertaining to different deformations while projecting on proton and neutron number then gives the energy surface from (2.42):

$$E\{\phi(\gamma, \beta, \varphi_N, \varphi_Z)\} = \frac{\langle\Psi|H|\Psi\rangle}{\langle\Psi|\Psi\rangle},$$

which is then minimized to give the result.

Not much difference is seen, but that is to be expected as $^{18}_{8}$O is near doubly magic; closed shells should give a spherical ground state and cause little pairing. Pairing of nucleons contributes little to the closed shells of the protons, while only two neutrons are free to pair amongst the neutrons.

This is also seen in the figure 3.8 where the norm of each state in the lattice is calculated after projection, that is

$$\langle\Phi|P_{N,Z}|\Phi\rangle\,,$$

for $N = 10$, $Z = 8$. The pairing interaction spreads the ground state into different multi-particle states with differing particle number, as seen in previous sections. For a pure (N,Z) state, with very well defined particle number, after projection should have a norm close to unity. Thus we can see from figure 3.8 that, for most of the states the contribution from the pairing interaction is small.

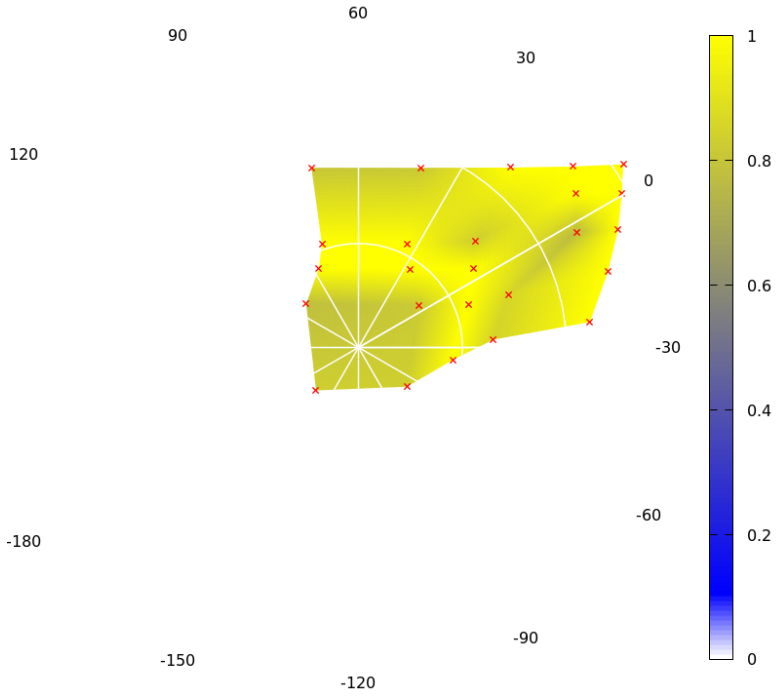

Figure 3.8: The projected norm of each individual state in the lattice. A value closer to 1 is indicative of low pairing, as the multi-body state is a pure $N = 10, Z = 8$ state.

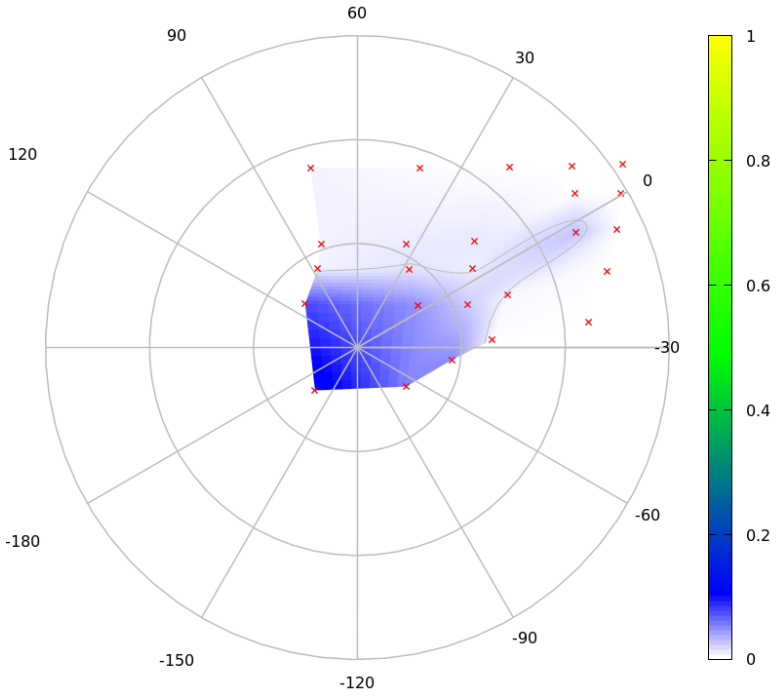

Figure 3.9: The projection of the GCM-ground state on each lattice state i.e. the weight or percentage of each lattice state found in the ground state.

In figure 3.9 the overlap of the spherical ground state $(\beta, \gamma) = (0, 0)$ with each state in the lattice is plotted. Clearly mostly the spherical states contribute, with some small contributions from the prolate shape. This is to be expected, as the ground state is clearly spherical in figure 3.7, caused by the fact that the nuclei is close to doubly magic.

Chapter 4

Conclusions and outlook

This thesis has investigated the effects of spontaneous symmetry breaking, and the restoration of said symmetries, in the superfluid states resulting from mean-field models of nuclei. The restoration of particle number symmetry, and to some extent angular momentum symmetry, using projection operators has been theoretically investigated. The details of which have been outlined for a model space using a BCS mean-field with seniority pairing but treated using Bogoliubov-Valantin quasi-particle formalism. This lead to the problem of calculating overlaps between quasi-particle vacuums, for which the approach using Pfaffians was investigated. Different algorithms for the computation of the Pfaffian, using routines found in the literature [1],[2], was tested for performance and accuracy. A computer program implementing a particle number projection operator for HFB-states, using the Pfaffian, was then implemented. This operator was then used to project out the particle number distribution $^{18}_{8}$O and $^{48}_{24}$Cr in the afore mentioned model space. The effects of truncating the model space, using two different methods, was investigated. Finally the particle number projection operator was then implemented in *HOSPHE* [3]. These calculations attempts to map phenomenologically motivated Skyrme-interactions (using SLy4 parametrization) to an effective Hamiltonian. Whose ground states were then approximated using configuration mixing of deformation and particle number, for which the particle number projection operator was used.

The results of Pfaffian performance tests gave pretty clear indications that the method of Householder rotations of [2] was to be preferred. This due to it fairing best in the runtime analysis and all methods were about equally accurate. The results seem pretty conclusive thus far, and further studies are not that well motivated. The authors of [14] has also published their version of Householder reflections which could be interesting to further investigate. Larger model spaces would also be of interest to use, as to the see if the computations scale as the results suggest.

Particle number projection clearly showed the distribution of particle number states present in the many-body state of the model space. It also showed that

closed shells are less affected by pairing interaction, which is accordance with experimental data [4]. For further studies the implementation of angular momentum would be of great interest, especially when studying heavier and more deformed nuclei.

The truncation of the model space gave inconclusive results and very much warrants further investigation. When doing so I would suggest using a much larger model space while also studying the U_α, V_α factors simultaneously. Maybe indicate what states α the truncation is affecting as to get a clear picture of the influence of the truncation. The results of [20] suggest a truncation for $V_\alpha^2 \approx 10^{-4}$ gives stable results for $N_{osc} = 18$.

Finally the results for the Skyrme-to-Hamiltonian calculations the results show great promise as the results are in accordance with experiment: a spherical ground state with little pairing interaction for $^{18}_{8}$O. Again, it would be interesting to implement the angular momentum projector to project out spin of the nucleus. One could also use said projector to find the excited rotational states for some nuclei.

Appendices

Appendix A

Occupation number formalism

A.1 Second Quantization

Let $\mathcal{H}$ be the hilbertspace of a single fermion system characterized by some hamiltonian $\hat{H}$. Furthermore let $\{|\alpha_k\rangle\}_0^\infty$ be the set of orthonormal eigenstates, thus corresponding to some quantum numbers of $\hat{H}$, such that

$$\hat{H}\,|\alpha_k\rangle = \varepsilon_k\,|\alpha_k\rangle\,. \tag{A.1}$$

The quantum numbers $|\alpha\rangle$ thus completely characterize the single fermion system and could for example be the oscillator basis $|nljm\rangle$. The wave function for particle i in state $|\alpha\rangle$ represented in $\bar{x}_i$-space, $\bar{x}_i = (\bar{r}_i, s_i)$, is written as

$$\langle \bar{x}_i|\alpha\rangle = \psi_\alpha(\bar{x}_i). \tag{A.2}$$

To describe a N-fermionic system the total wave function has to obey the Pauli-principle which gives anti-symmetric states for a fermionic system. To construct a set of such basis functions let n_α denote the number of particles in state α. According to the Pauli-principle n_α can only take the values 0 or 1 as no single state can be occupied by more than one fermion. Using these occupation numbers the N-particle basis wave functions can be expressed as

$$\Phi_{\{n_\alpha\}}(1,\ldots,N) = \frac{1}{\sqrt{N!}} \sum_{P\in S_N} \mathrm{sign}(P) P\{\psi_{\alpha_1}\cdot\ldots\cdot\psi_{\alpha_N}\}. \tag{A.3}$$

In occupation number formalism the single particle states are ordered in increasing energy (just like above) and written as

$$|n_1, n_2, \ldots, n_N\rangle = |\alpha_1, \alpha_2, \ldots, \alpha_N\rangle\,. \tag{A.4}$$

The N-particle basis states $\Phi_{\{n_\alpha\}}$ or $|n_1,\ldots,n_N\rangle$ thus span a space called the Fock space $\mathcal{F}$. $\mathcal{F}$ should thus contain all the single fermion states in $\mathcal{H}_1$, two fermionic

states in $\mathcal{H}_2$, and so on – but also the zero particle state-space $\mathcal{H}_0 = \mathbb{C}$, i.e.

$$\mathcal{F} = \mathbb{C} \oplus \mathcal{H}_1 \oplus \mathcal{H}_2 \oplus \cdots = \bigoplus_{n=0}^{\infty} \mathcal{H}_n. \tag{A.5}$$

The zero particle state, or vacuum state, is written as

$$|0\rangle = |0_1, 0_2, \ldots\rangle\,, \tag{A.6}$$

and the fermion creation operator $\hat{c}_i^\dagger$ is defined as

$$\hat{c}_i^\dagger\,|0\rangle = (-1)^{\sum_{j<i} n_j}\,|n_1, n_2, \ldots, 1_i, \ldots\rangle\,, \qquad \hat{c}_i^\dagger\,|n_1, n_2, \ldots, 1_i, \ldots\rangle = 0. \tag{A.7}$$

The Hermitian conjugate of the creation operator is called the annihilation operator $(\hat{c}_{\alpha_i}^\dagger)^\dagger = \hat{c}_{\alpha_i}$ defined as

$$\hat{c}_i\,|n_1, n_2, \ldots, 1_i, \ldots\rangle = (-1)^{\sum_{j<i} n_j}\,|n_1, n_2, \ldots, 0_i, \ldots\rangle\,, \qquad \hat{c}_i\,|n_1, n_2, \ldots, 0_i, \ldots\rangle = 0. \tag{A.8}$$

Note that these operators are indeed mappings between the different subspaces of $\mathcal{F}$;

$$\hat{c}_i : \mathcal{H}_N \to \mathcal{H}_{N-1},$$
$$\hat{c}_i^\dagger : \mathcal{H}_N \to \mathcal{H}_{N+1}.$$

Consequently they can be represented using anti-symmetric tensor products ($\otimes_-$)

$$\hat{c}_i^\dagger \Phi_{\{n_\alpha\}} = \frac{1}{\sqrt{N+1}} \psi_{\alpha_i} \otimes_- \Phi_{\{n_\alpha\}}, \tag{A.9}$$

and some Using these operators

$$|n_1, \ldots, n_{\alpha_N}, \ldots\rangle = \prod_\mu (\hat{c}_\mu^\dagger)^{n_\mu}\,|0\rangle = \hat{c}_{\alpha_1}^\dagger \hat{c}_{\alpha_2}^\dagger \ldots |0\rangle \tag{A.10}$$

The operators also obey the following anti-commutator relations;

$$\{\hat{c}_i, \hat{c}_j^\dagger\} = \hat{c}_i \hat{c}_j^\dagger + \hat{c}_j^\dagger \hat{c}_i = \delta_{i,j},$$
$$\{\hat{c}_i, \hat{c}_j\} = \{\hat{c}_i^\dagger, \hat{c}_j^\dagger\} = 0.$$

Noting the fact that the first anti-commutator relation gives

$$\hat{c}_j^\dagger \hat{c}_i\,|\ldots, n_i, \ldots\rangle = n_i \delta_{i,j}\,|\ldots, n_i, \ldots\rangle\,, \tag{A.11}$$

the number operator is identified:

$$\hat{N} = \sum_{i=1}^{N} \hat{c}_i^\dagger \hat{c}_i = \sum_{i=1}^{N} \hat{n}_i,$$
$$\hat{N}\,|n_1, n_2, \ldots\rangle = N\,|n_1, n_2, \ldots\rangle\,.$$

A simple proof for the first anti-commutator relation:

$$\begin{aligned}\hat{c}_i\hat{c}_j^\dagger \left|\ldots, n_i, \ldots, n_j, \ldots\right\rangle &= \hat{c}_i\theta_j n_j \left|\ldots, n_i, \ldots, 1_j, \ldots\right\rangle \\ &= \theta_j\theta_i n_i n_j \left|\ldots, 0_i, \ldots, 1_j, \ldots\right\rangle \\ &= \delta_{i,j},\end{aligned}$$

the same is true for the reverse order of the operators Q.E.D.

A simple proof of the second anti-commutator relation:

$$\begin{aligned}\hat{c}_i\hat{c}_j \left|\ldots, n_i, \ldots, n_j, \ldots\right\rangle &= \hat{c}_i\theta_j n_j \left|\ldots, n_i, \ldots, 0_j, \ldots\right\rangle \\ &= \theta_j\theta_i n_j n_i \left|\ldots, 0_i, \ldots, 0_j, \ldots\right\rangle,\end{aligned}$$

while

$$\begin{aligned}\hat{c}_j\hat{c}_i \left|\ldots, n_i, \ldots, n_j, \ldots\right\rangle &= \hat{c}_j\theta_i n_i \left|\ldots, n_i, \ldots, 0_j, \ldots\right\rangle \\ &= (-1)^{0-n_i}\theta_i\theta_j n_i n_j \left|\ldots, 0_i, \ldots, 0_j, \ldots\right\rangle \\ &= -\theta_i\theta_j n_i n_j \left|\ldots, 0_i, \ldots, 0_j, \ldots\right\rangle,\end{aligned}$$

Q.E.D.

A.2 Operator representation in second quantization

The matrix representation of a single particle operator is generally, for any complete sets $|\alpha\rangle$, $|\beta\rangle$;

$$\hat{F} = \sum_{\alpha,\beta} |\alpha\rangle \langle\alpha| F |\beta\rangle \langle\beta| . \tag{A.12}$$

A single particle operator in a N-body system, $\hat{F_N}$, can be written as the sum of the single particle operators, $\hat{F}_i$ acting on each particle i;

$$\hat{F}_N = \sum_{i=1}^{N} \hat{F}_i. \tag{A.13}$$

In the occupation number formalism the single particle operators act on the corresponding particle state;

$$\begin{aligned}\hat{F}_i \left|n_1, n_2, \ldots, n_i, \ldots\right\rangle &= \hat{F}_i \left|\alpha_1, \alpha_2, \ldots, \alpha_i, \ldots\right\rangle, \\ &= \sum_{\beta_i} \langle\beta_i| F |\alpha_i\rangle \left|\alpha_1, \alpha_2, \ldots, \beta_i, \ldots\right\rangle .\end{aligned}$$

using equation above. This means that the total action of a single particle operator can be stated as;

$$\begin{aligned}\hat{F}_N \left|\alpha_1, \alpha_2, \ldots, \alpha_i, \ldots\right\rangle &= \sum_{i=1}^{N} \hat{F}_i \left|\alpha_1, \alpha_2, \ldots, \alpha_i, \ldots\right\rangle, \\ &= \sum_{i=1}^{N} \sum_{\beta_i} \left\langle\beta_i\right| F \left|\alpha_i\right\rangle \left|\alpha_1, \alpha_2, \ldots, \beta_i, \ldots\right\rangle.\end{aligned}$$

Using the creation and annihilation operators a different representation of $\hat{F}_N$ in $\mathcal{F}$ is possible;

$$\hat{F}_{\mathcal{F}} = \sum_{\alpha,\beta} \left\langle\alpha\right| F \left|\beta\right\rangle \hat{c}^{\dagger}_{\alpha} \hat{c}_{\beta}. \tag{A.14}$$

To prove their equivalence, the commutator can be used. Evaluating the action of $\hat{F}_{\mathcal{F}}$ gives

$$\begin{aligned}\hat{F}_{\mathcal{F}} \left|\alpha_1, \alpha_2, \ldots, \alpha_N, \ldots\right\rangle &= \hat{F}_{\mathcal{F}} \hat{c}^{\dagger}_{\alpha_1} \hat{c}^{\dagger}_{\alpha_2} \ldots \hat{c}^{\dagger}_{\alpha_N} \left|0\right\rangle \\ &= [\hat{F}_{\mathcal{F}}, \hat{c}^{\dagger}_{\alpha_1}] \hat{c}^{\dagger}_{\alpha_2} \ldots \hat{c}^{\dagger}_{\alpha_N} \left|0\right\rangle + \hat{c}^{\dagger}_{\alpha_1} \hat{F}_{\mathcal{F}} \hat{c}^{\dagger}_{\alpha_2} \ldots \hat{c}^{\dagger}_{\alpha_N} \left|0\right\rangle \\ &= [\hat{F}_{\mathcal{F}}, \hat{c}^{\dagger}_{\alpha_1}] \hat{c}^{\dagger}_{\alpha_2} \ldots \hat{c}^{\dagger}_{\alpha_N} \left|0\right\rangle + \hat{c}^{\dagger}_{\alpha_1} [\hat{F}_{\mathcal{F}}, \hat{c}^{\dagger}_{\alpha_2}] \hat{c}^{\dagger}_{\alpha_2} \ldots \hat{c}^{\dagger}_{\alpha_N} \left|0\right\rangle \\ &\quad + \ldots + \hat{c}^{\dagger}_{\alpha_1} \hat{c}^{\dagger}_{\alpha_2} \ldots [\hat{F}_{\mathcal{F}}, \hat{c}^{\dagger}_{\alpha_N}] \left|0\right\rangle \\ &= \sum_{i=1}^{N} \sum_{\beta_i} \left\langle\beta_i\right| \hat{F} \left|\alpha_i\right\rangle \hat{c}^{\dagger}_{\alpha_1} \ldots \hat{c}^{\dagger}_{\beta_i} \ldots \hat{c}_{\alpha_N} \left|0\right\rangle \\ &= \sum_{i=1}^{N} \sum_{\beta_i} \left\langle\beta_i\right| \hat{F} \left|\alpha_i\right\rangle \left|\alpha_1, \alpha_2, \ldots, \beta_i, \ldots\right\rangle.\end{aligned}$$

This proves that the two matrices have the same action and since the representation holds for any N the two operators must be equivalent.

The matrix elements of the single particle operator can generally be expressed as

$$\begin{aligned}\left\langle\beta\right| \hat{F} \left|\alpha\right\rangle &= \int d\mathbf{x} \int d\mathbf{x}' \left\langle\alpha|\mathbf{x}\right\rangle \left\langle\mathbf{x}\right| \hat{F} \left|\mathbf{x}'\right\rangle \left\langle\mathbf{x}'|\beta\right\rangle, \\ &= \int d\mathbf{x}\, \psi_{\alpha}(\mathbf{x})^{*} \hat{F}(\mathbf{x}) \psi_{\beta}(\mathbf{x})\end{aligned}$$

A general two particle operator in Fock-space is then given as;

$$\hat{V} = \sum_{i<j=1}^{N} \hat{v}_{ij} = \frac{1}{2} \sum_{i \neq j} \hat{v}(\mathbf{x}_i, \mathbf{x}_j) = \frac{1}{2} \sum_{\alpha\beta\delta\gamma} v_{\alpha\beta\delta\gamma} \hat{c}^{\dagger}_{\alpha} \hat{c}^{\dagger}_{\beta} \hat{c}_{\delta} \hat{c}_{\gamma} \tag{A.15}$$

with the matrix element

$$v_{\alpha\beta\delta\gamma} = \int d^3\mathbf{x} \int d^3\mathbf{x}'\, \psi_{\alpha}(\mathbf{x})^{*} \psi_{\beta}(\mathbf{x}')^{*} \hat{v}(\mathbf{x}, \mathbf{x}') \psi_{\delta}(\mathbf{x}) \psi_{\gamma}(\mathbf{x}'). \tag{A.16}$$

Defining the anti-symmetrized matrix elment $\bar{v}_{\alpha\beta\delta\gamma}$ as:

$$\bar{v}_{\alpha\beta\delta\gamma} = v_{\alpha\beta\delta\gamma} - v_{\alpha\beta\gamma\delta}, \tag{A.17}$$

Bibliography

[1] C. González-Ballestero, L.M. Robledo, and G.F. Bertsch. "Numeric and symbolic evaluation of the pfaffian of general skew-symmetric matrices". In: *Computer Physics Communications* 182.10 (2011), pp. 2213–2218. ISSN: 0010-4655. DOI: https://doi.org/10.1016/j.cpc.2011.04.025.

[2] M. Wimmer. "Algorithm 923: Efficient Numerical Computation of the Pfaffian for Dense and Banded Skew-Symmetric Matrices". In: *ACM Trans. Math. Softw.* 38.4 (Aug. 2012), 30:1–30:17. ISSN: 0098-3500. DOI: 10.1145/2331130.2331138.

[3] B. G. Carlsson et al. "Solution of self-consistent equations for the N^{3}LO nuclear energy density functional in spherical symmetry. The program HOSPHE (v1.02)." English. In: *Comput. Phys. Commun.* 181.9 (2010), pp. 1641–1657. ISSN: 0010-4655.

[4] P. Ring and P. Schuck. *The Nuclear Many-Body Problem*. Physics and astronomy online library. Springer, 2004. ISBN: 9783540212065. URL: https://books.google.se/books?id=PTynSM-nMA8C.

[5] I. Ragnarsson and S.G. Nilsson. *Shapes and Shells in Nuclear Structure*. Cambridge University Press, 2005. ISBN: 9780521019668. URL: https://books.google.se/books?id=G1FhlKtxbtUC.

[6] Morton Hamermesh. *Group Theory and Its Application to Physical Problems (Dover Books on Physics)*. Dover Publications, 1989. ISBN: 0486661814.

[7] J. A. Sheikaaaah et al. "Symmetry restoration in mean-field approaches". In: *arXiv e-prints* (Jan. 2019). arXiv: 1901.06992 [nucl-th].

[8] J.L. Egido and P. Ring. "Symmetry conserving Hartree-Fock-Bogoliubov theory: (I). On the solution of variational equations". In: *Nuclear Physics A* 383.2 (1982), pp. 189–204. ISSN: 0375-9474. DOI: https://doi.org/10.1016/0375-9474(82)90447-X.

[9] J.J. Sakurai and J. Napolitano. *Modern Quantum Mechanics*. Addison-Wesley, 2011. ISBN: 9780805382914.

[10] David Lawrence Hill and John Archibald Wheeler. "Nuclear Constitution and the Interpretation of Fission Phenomena". In: *Phys. Rev.* 89 (5 Mar. 1953), pp. 1102–1145. DOI: 10.1103/PhysRev.89.1102.

[11] James J. Griffin and John A. Wheeler. "Collective Motions in Nuclei by the Method of Generator Coordinates". In: *Phys. Rev.* 108 (2 Oct. 1957), pp. 311–327. DOI: 10.1103/PhysRev.108.311.

[12] Naoki Onishi and Shiro Yoshida. "Generator coordinate method applied to nuclei in the transition region". In: *Nuclear Physics* 80.2 (1966), pp. 367–376. ISSN: 0029-5582. DOI: https://doi.org/10.1016/0029-5582(66)90096-4.

[13] Shingo Tagami and Yoshifumi R. Shimizu. "Efficient Method to Perform Quantum Number Projection and Configuration Mixing for Most General Mean-Field States". In: *Progress of Theoretical Physics* 127.1 (Jan. 2012), pp. 79–115. ISSN: 0033-068X. DOI: 10.1143/PTP.127.79. eprint: http://oup.prod.sis.lan/ptp/article-pdf/127/1/79/19572858/127-1-79.pdf.

[14] G. F. Bertsch and L. M. Robledo. "Symmetry Restoration in Hartree-Fock-Bogoliubov Based Theories". In: *Phys. Rev. Lett.* 108 (4 Jan. 2012), p. 042505. DOI: 10.1103/PhysRevLett.108.042505.

[15] Zao-Chun Gao, Qing-Li Hu, and Y.S. Chen. "A convenient implementation of the overlap between arbitrary Hartree–Fock–Bogoliubov vacua for projection". In: *Physics Letters B* 732 (2014), pp. 360–363. ISSN: 0370-2693. DOI: https://doi.org/10.1016/j.physletb.2014.04.012.

[16] V N Fomenko. "Projection in the occupation-number space and the canonical transformation". In: *Journal of Physics A: General Physics* 3.1 (Jan. 1970), pp. 8–20. DOI: 10.1088/0305-4470/3/1/002. URL: https://doi.org/10.1088/0305-4470/3/1/002.

[17] Michael Bender, Paul-Henri Heenen, and Paul-Gerhard Reinhard. "Self-consistent mean-field models for nuclear structure". In: *Rev. Mod. Phys.* 75 (1 Jan. 2003), pp. 121–180. DOI: 10.1103/RevModPhys.75.121.

[18] Takahiro Mizusaki, Makito Oi, and Noritaka Shimizu. "Why does the sign problem occur in evaluating the overlap of HFB wave functions?" In: *Physics Letters B* 779 (2018), pp. 237–243. ISSN: 0370-2693. DOI: https://doi.org/10.1016/j.physletb.2018.02.012.

[19] Takahiro Mizusaki and Makito Oi. "A new formulation to calculate general HFB matrix elements through the Pfaffian". In: *Physics Letters B* 715.1 (2012), pp. 219–224. ISSN: 0370-2693. DOI: https://doi.org/10.1016/j.physletb.2012.07.023.

[20] Shingo Tagami and Yoshifumi R. Shimizu. "Efficient Method to Perform Quantum Number Projection and Configuration Mixing for Most General Mean-Field States". In: *Progress of Theoretical Physics* 127.1 (Jan. 2012), pp. 79–115. ISSN: 0033-068X. DOI: 10.1143/PTP.127.79.

[21] E. Chabanat et al. "A Skyrme parametrization from subnuclear to neutron star densities Part II. Nuclei far from stabilities". In: *Nuclear Physics A* 635.1 (1998), pp. 231–256. ISSN: 0375-9474. DOI: https://doi.org/10.1016/S0375-9474(98)00180-8.

[22] E. Chabanat et al. "A Skyrme parametrization from subnuclear to neutron star densities". In: *Nuclear Physics A* 627.4 (1997), pp. 710–746. ISSN: 0375-9474. DOI: https://doi.org/10.1016/S0375-9474(97)00596-4.